

Article

Temperature Impact on the Assessment of Reinforcement Corrosion Risk in Concrete by Galvanostatic Pulse Method

Wioletta Raczkiwicz *  and Artur Wójcicki

Kielce University of Technology, Faculty of Civil Engineering and Architecture, Al. Tysiąclecia Państwa Polskiego 7, 25-314 Kielce, Poland; arturw@tu.kielce.pl

* Correspondence: wioLAR@tu.kielce.pl; Tel.: +48-4134-24-582

Received: 10 December 2019; Accepted: 1 February 2020; Published: 6 February 2020



Abstract: The electrochemical galvanostatic pulse method (GPM) is used for the evaluation of the degree of corrosion risk of reinforcement in concrete. This non-destructive method enables determining the corrosion promoting conditions through the measurements of reinforcement stationary potential and concrete cover resistivity, and determining the probability of reinforcement corrosion in the tested areas. This method also allows for the estimation of the reinforcement corrosion activity and the prediction of the development of the corrosion process on the basis of corrosion current density measurements. The ambient temperature (and the temperature of the examined element) can significantly affect the values of the measured parameters due to electrochemical character of the processes as well as specific measurement technique. Differences in the obtained results can lead to a wrong interpretation of reinforcement corrosion risk degree in concrete. The article attempts to assess the effect of temperature on the measured parameters while using the galvanostatic pulse method. The GP-5000 GalvaPulse™ set was used. The results of this study confirmed the impact of temperature changes on the values of three measured parameters (reinforcement stationary potential, concrete cover resistivity, and corrosion current density) and contributed to catching the trend of these changes.

Keywords: reinforced concrete diagnostics; non-destructive method; galvanostatic pulse method; reinforcement corrosion; temperature impact

1. Introduction

Durability is one of the main requirements for building structures [1–5]. In the steel and reinforced concrete structures, the steel corrosion is a direct factor that affects durability of concrete [2–7]. While in steel structures, corrosion protective coatings are usually visible, and the corrosion process itself is relatively easy to notice and evaluate, in reinforced concrete structures, the corrosion of the reinforcement will be undetected on the surface of concrete for many years, thus causing significant destruction and making corrosion assessment more difficult. However, there is a group of non-destructive methods that allow, in probabilistic terms, diagnosing the process of reinforcement corrosion in a structural element [6–12]. These are electrochemical methods that utilize the physico-chemical properties of concrete and steel. Small gel pores, larger capillary pores, and macro-pores form the porous structure of concrete, which form a system of interconnected channels that are filled with ion-carrying liquid. Steel reinforcing bars, on the other hand, are electron carriers. The flow of electrons between the existing local anode and cathode microcells (resulting from microdefects in steel) on the bar surface and the ion flow in the liquid filling the pores of concrete produce a kind of galvanic cell. The alkaline liquid in the pores is an electrolyte and the reinforcing bar is an electrode [6,13–15]. Reinforcement corrosion begins

in favourable conditions, when the passive layer protecting the bar surface is damaged (usually as a result of concrete carbonation or action of chlorides), the pores are filled with liquid, and oxygen is available. The iron oxidation process occurs at the anode:



and the reduction process occurs at the cathode:

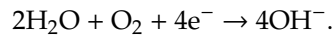


Figure 1 schematically this.

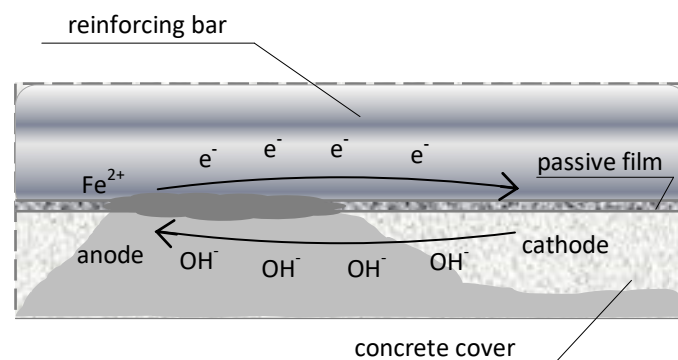
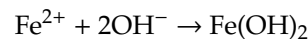
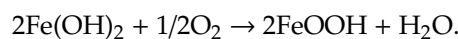


Figure 1. Reinforcement corrosion process in concrete.

In the course of the corrosion process, iron ions react with OH^{-} ions, forming iron hydroxide:



and then in the presence of oxygen:



As a result of the process, iron hydroxide is formed $\text{Fe}(\text{OH})_3$ and iron oxide Fe_2O_3 are produced. The corrosion product, rust, is a mixture of $\text{Fe}(\text{OH})_3$, Fe_2O_3 , Fe_3O_4 , H_2O , and magnetite [2,6,13,14]. The degree of reinforcing bar corrosion can be determined from Equation (1) by calculating the corrosion loss that is based on Faraday’s law:

$$\Delta m = k \times i \times t \tag{1}$$

where:

- Δm —loss of weight [g],
- K —electrochemical equivalent [g/A × s]
- i —corrosive current strength [A], and
- t —current flow time [s].

The corrosive current can be determined from Equation (2):

$$i = \frac{\Delta E}{R_K + R_A + R_O + R_Z} \tag{2}$$

where:

- ΔE —anode and cathode potential difference,
- R_K, R_A —cathode and anode polarization resistance, and
- R_O, R_Z —internal and external circuit resistance.

Equation (2) indicates that the moisture level-dependent internal resistance that inhibits ion transport is important. The diffusion is practically stopped at the moisture content below 75%.

The temperature of the tested element also affects the ion diffusion coefficient [2,13]. The diffusion coefficient increases with the increase in temperature (the increase rate depends on the concrete composition), as shown by the Arrhenius equation:

$$D = D_0 e^{-\frac{E}{RT}} \quad (3)$$

where:

D–diffusion coefficient at temperature T [cm²/s],

D₀–diffusion coefficient at temperature T = 0,

E–activation energy of the diffusion process [kJ/mol] (dependent on w/c and type of cement),

R–gas constant (R = 8.3144598(48) [J/mol × K]), and

T–absolute temperature [K].

As a result of the electrochemical process of reinforcement corrosion in concrete, certain electrical quantities change. Stationary potential, concrete resistivity, or corrosion current density can be measured and used for the estimation of the extent of reinforcement corrosion. Measurements are made while using specialized devices and the results are analyzed against the criteria values pre-determined for a given device [6,12,16–32]

The galvanostatic pulse method (GPM) is one of the methods used for this purpose [21–32]. It is a non-destructive polarization technique that allows for measurements of the reinforcement stationary potential on the concrete surface (E_{st}), concrete cover resistivity (Θ), and corrosion current density (i_{cor}). The measurements of the reinforcement stationary potential and the concrete cover resistivity are called basic measurements. It should be noted that the values of the reinforcement stationary potential and the concrete cover resistivity are only estimates of the probability of reinforcement corrosion risk in the investigated areas, and the measurement results are not meaningful. Corrosive current density data, on the other hand, allow for the estimation of corrosion activity in the reinforcement and prediction of its rate over time. The dynamic equilibrium on the electrode (reinforcing bar) immersed in the electrolyte (alkaline liquid filling the pores) has to be disturbed (polarization of the reinforcement) to conduct the measurements. In the case of the galvanostatic pulse method, a current of certain intensity generates such a disturbance.

External factors, including electrolyte temperature, have some influence on the intensity of the process due to the fact that ions flow as a result of diffusion in the pore liquid, and thus also on the measured electrical values. As reported by Neville [2], the diffusion coefficient (D) increases as the electrolyte temperature increases (3), which is directly related to the ion flow rate in the electrolyte and the measurement of this flow. In addition, the increase in temperature accelerates depolarization, which is important when galvanostatic pulse measurements are used. Although the galvanostatic pulse method has been used for several years [21–31], few authors have evaluated the impact of temperature on the measurement results [20,23,25,28,30,31]. Most research has been devoted to the impact of environmental conditions, i.e., both temperature and moisture content. Little or no information regarding the possible correlation between the temperature of the tested element and the obtained measurement results can be found in the literature, which suggests that it is not taken into account.

The authors' previous research [21,25,28] prompted the thesis that the temperature of the tested element has a significant impact on the values of the measured parameters, which is also indicated by the physico-chemical nature of the reinforcement corrosion process in concrete. The results of measurements that were made on the same laboratory specimen, both outdoors in winter (in temperature of about 0 °C) and indoors at room temperature (about 23 °C), varied noticeably [25,28]. Similar observations of differences in the corrosion rates between September 2000 and April 2001 were reported in [23]. For this reason, tests were carried out on a larger number of samples under gradually changed thermal conditions. The purpose of the work was to determine an influence of the temperature of the tested element on the measurement results of three parameters: the corrosion

current density, the reinforcement stationary potential, and the concrete cover resistivity. The influence of temperature on the results of potential and resistivity measurements may result in incorrect marking of areas for advanced measurements and, as a consequence, disturb corrosion risk assessment, although measurements of stationary reinforcement potential and concrete cover resistivity are less important than measurements of corrosive current density in general GPM tests. Analysis of the values of these parameters allows for the estimation of actual steel reinforcement corrosion degree.

2. Measuring Device

The GP-5000 GalvaPulse™ set is one of the devices designed to measure stationary reinforcement potential and concrete cover resistivity (basic measurements) or, additionally, corrosion current density (advanced measurements) while using the polarization method [32]. The half-cell potential is measured to an accuracy of ± 5 mV with the Ag/AgCl electrode. The electrical resistance is estimated to be measured with an accuracy of $\pm 5\%$ [32]. The main elements of the set include the control and recording device (PSION minicomputer), silver-chloride reference electrode (Ag/AgCl), and calibration device (Figure 2).



Figure 2. The GP-5000 GalvaPulse™ set.

The GP-5000 GalvaPulse™ can be used in both laboratory and field conditions. Measurements are made on the surface of the element at the points evenly distributed above the reinforcement. This allows for creating graphical maps of the distribution of measured parameters and facilitates further comprehensive analysis of the results, especially for large-size elements. For the measurements, the reinforcing bar (local hole is required) is connected with the calibrated control and recording device (PSION minicomputer) and with the reference electrode.

Before the measurements, the location of the tested bar is determined and its continuity along the tested section is checked. Where the electrode is applied, the concrete surface must be properly cleaned and wetted. The recommended concrete resistivity should be no more than $50 \text{ k}\Omega\cdot\text{cm}$. Changes in the moisture content in concrete result in resistivity changes, which, at a given constant current strength, could lead to incorrect measurements of the reinforcement stationary potential. Therefore, the moisture concentration on the tested surface should be maintained as constant throughout the measurement period. Figure 3 shows the connection scheme of the GP-5000 GalvaPulse™ set with the tested reinforcement.



Figure 3. The connection scheme of the GP-5000 GalvaPulse™ set with the tested reinforcement.

The measuring device must be properly calibrated by entering the coordinates of the measurement points on the test surface, pulse duration ($5 \div 20$ s), current strength ($5 \div 400 \mu\text{A}$; a higher value is expected for bigger quantity of corrosion products), reinforcing bar parameters (diameter, length, surface area), and by activating (if necessary) the ring that limits the electrode area of operation.

Information on the criteria for the interpretation of the test results is attached to the apparatus (Table 1). It is possible to infer about the probability of reinforcement corrosion in the examined area, and the corrosion process rate can be estimated based on the value of the corrosion current density, depending on the obtained values of the reinforcement stationary potential and the concrete cover resistivity. Table 1 summarizes the appropriate criteria for measurements performed while using a GP-5000 GalvaPulse™ set. The reference values should not be compared with the measurements that were obtained with other devices [6,32].

Table 1. Criteria for assessing the reinforcement corrosion risk level [32].

Criteria for Assessing the Degree of Reinforcement Corrosion Risk by use a GP-5000 GalvaPulse™ Set			
	Reinforcement Corrosion Activity, $i_{\text{cor}}[\mu\text{A}/\text{cm}^2]$		Corrosion Rate, [mm/year]
Corrosion current density	<0.5	not forecasted corrosion activity	<0.006
	0.5 ÷ 2.0	irrelevant corrosion activity	0.006 ÷ 0.023
	2.0 ÷ 5.0	low corrosion activity	0.023 ÷ 0.058
	5.0 ÷ 15.0	moderate corrosion activity	0.058 ÷ 0.174
	>15.0	high corrosion activity	>0.174
Reinforcement stationary potential, E_{st} [mV] vs. Ag/AgCl	<−350		95% of corrosion probability
	−350 ÷ −200		50% of corrosion probability
	>−200		5% of corrosion probability
Concrete cover resistivity, Θ [k Ω ·cm]	≤ 10		high corrosion probability
	10 ÷ 20		medium corrosion probability
	≥ 20		small corrosion probability

3. Research Methodology and Material

Seven rectangular specimens with dimensions $210 \times 228 \times 100$ mm were cast. The specimens were made from the same concrete mixture (C40/45) under identical laboratory conditions. The following quantities of constituents were assumed for 1 m^3 of the mixture: cement (CEM I 52.5) – 390 kg, sand – 660 kg, aggregate $2 \div 8$ – 617 kg, aggregate $8 \div 16$ – 694 kg, water – 155 L, plasticizer (1.84 g), and

air-entraining admixture (0.47 g). Two parallel ribbed bars with a diameter of 8 mm that were made of BST 500 steel were placed in each specimen 70 mm from the side edges and 25 mm from the upper specimen surface – the cover (Figure 4). The specimens were stored at a temperature of $20\text{ }^{\circ}\text{C} \pm 2\text{ }^{\circ}\text{C}$, and relative humidity of $50\% \pm 5\%$.



Figure 4. The test specimen.

An orthogonal grid of four measuring points was established for measurement purposes, being spaced evenly every 70 mm on each specimen (two points above each bar) in which reinforcement stationary potential, concrete cover resistivity and corrosion current density were measured (Figure 5). The measurements were carried out in accordance with the requirements of the GP-5000 GalvaPulse™ use. The obtained results were archived in the created database.



Figure 5. Photo of measurements carried out on one of the tested specimens.

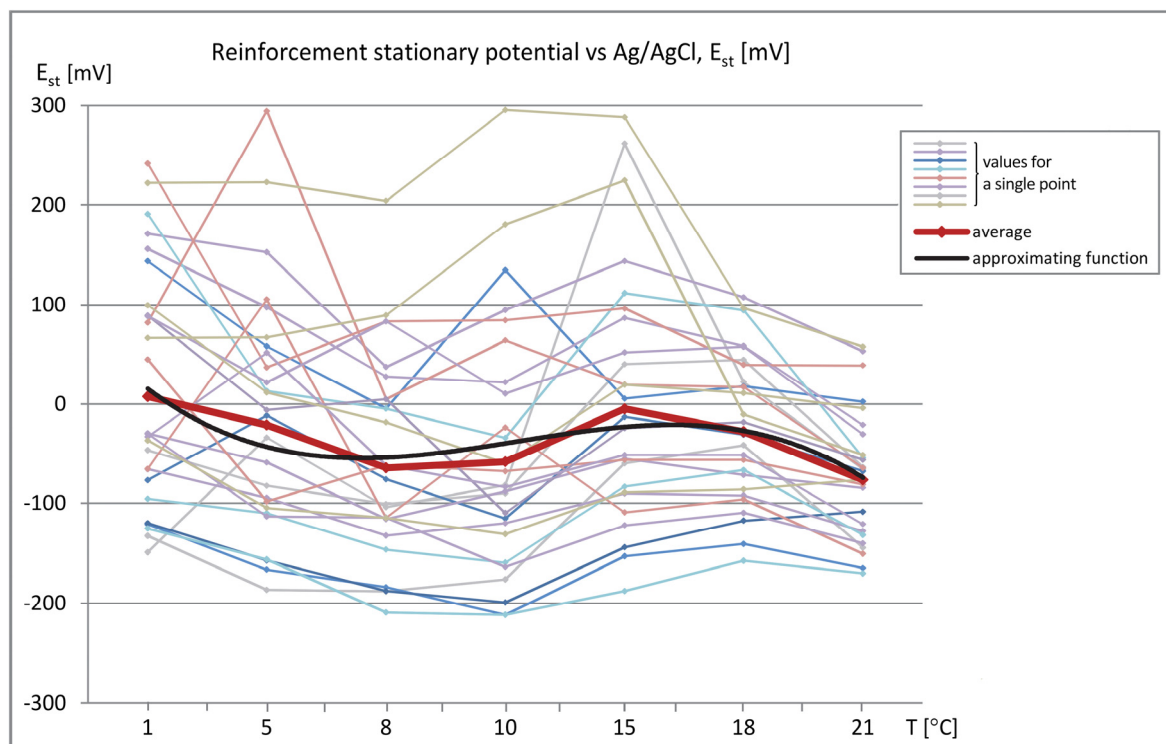
The test temperatures were varied and they included $1\text{ }^{\circ}\text{C}$, $5\text{ }^{\circ}\text{C}$, $8\text{ }^{\circ}\text{C}$, $10\text{ }^{\circ}\text{C}$, $15\text{ }^{\circ}\text{C}$, $18\text{ }^{\circ}\text{C}$, and $21\text{ }^{\circ}\text{C}$. The choice of temperature range resulted from the intention to reflect the real conditions in which in-situ research is usually carried out. Measurements were not possible at minus temperatures due to the specifics of the measurement technique, i.e., the use of the electrolysis process and the need for strong hydration of the concrete surface in the studied area. The temperature of specimen surface was measured every time at three points while using a non-contact infrared thermometer with a range of $-50\text{ }^{\circ}\text{C} \div 380\text{ }^{\circ}\text{C}$ and tolerance of $\pm 0.5\text{ }^{\circ}\text{C}$.

4. Research Results and the Analysis

The data sets of the measured parameters (reinforcement stationary potential- E_{st} , concrete cover resistivity- Θ , and corrosion current density- i_{cor}) as a function of temperature were produced, as shown in Figure 6 (measured values) and Figure 7 (relative values referred to the values measured at $T = 1\text{ }^{\circ}\text{C}$). The graphs show the relation between the obtained results and the specimen temperature.

Analysis of the values of parameters determining the probability of reinforcement corrosion in the examined region, i.e., reinforcement stationary potential (E_{st}) and concrete cover resistivity (Θ), showed that the obtained values were in the ranges: $E_{st} = -212 \div 295\text{ mV}$ and $\Theta = 5.3 \div 57.5\text{ k}\Omega\cdot\text{cm}$. As described earlier, the measurements were made on the same specimens at the same measuring points, but at varied temperature values. While the values of reinforcement stationary potential at almost all assumed temperatures were less than -200 mV , which indicated the same 5% probability of reinforcement corrosion in the tested region (although with a wide spread of results), the values of concrete cover resistivity exhibited relatively high variability and, thus, led to significantly different conclusions about the corrosion probability—from low to high. Thus the temperature of the concrete cover has a large impact on its resistivity. The results of the third measured parameter, i.e., corrosion current density, were in the range of irrelevant corrosion activity, $i_{cor} = 0.18 \div 1.0\text{ }\mu\text{A}/\text{cm}^2$, which corresponded to the real condition of the tested specimens.

In addition, at a given measurement point for a given parameter, the changes in its value versus temperature were quite similar. This indicates a constant (though not equally significant) effect of specimen temperature on the obtained values of the measured parameter. The values were averaged in order to discover the global trend of changes in the value of each parameter, as shown in Figure 6. The plot of average values is marked with a red thick line, whereas the black thin line denotes the approximating function in the form of a three-degree polynomial.



(a)

Figure 6. Cont.

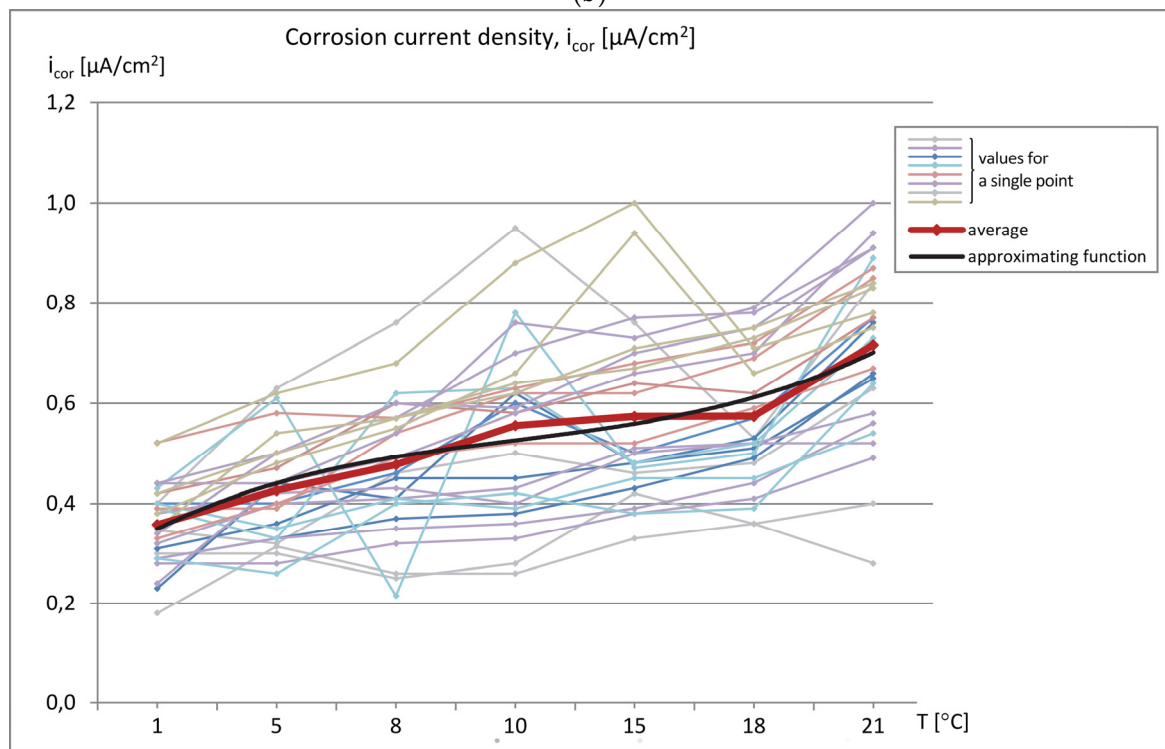
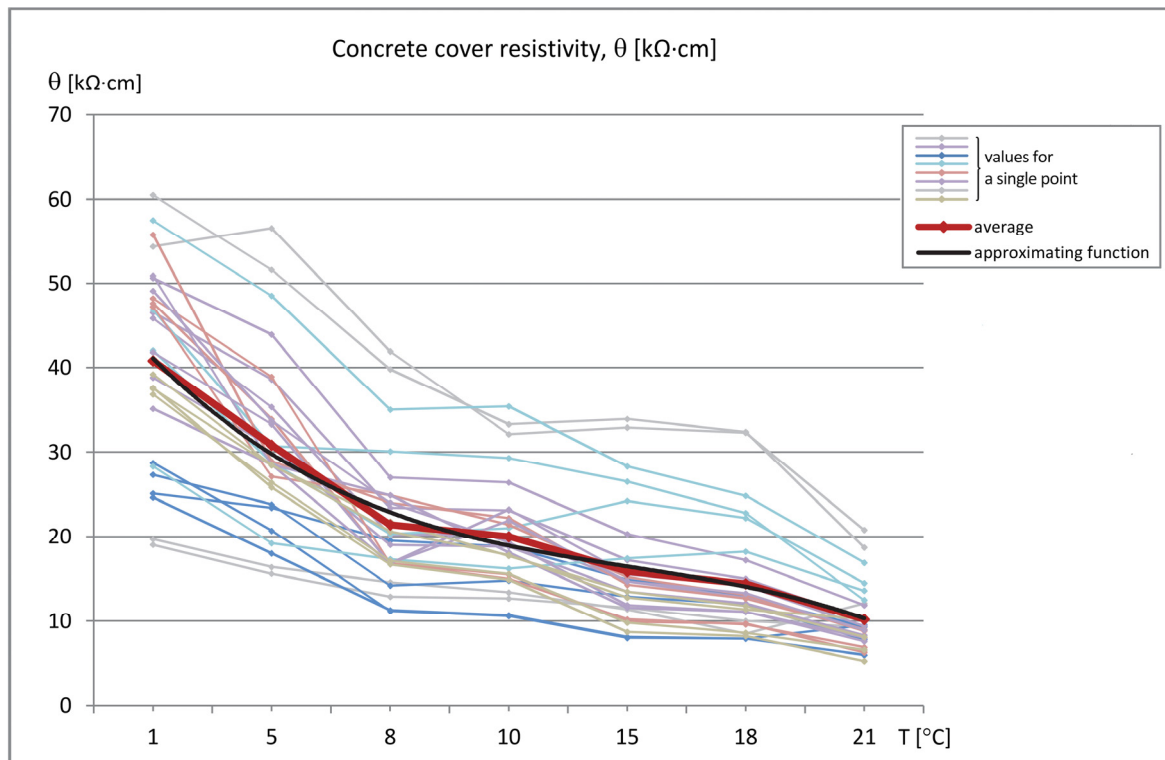
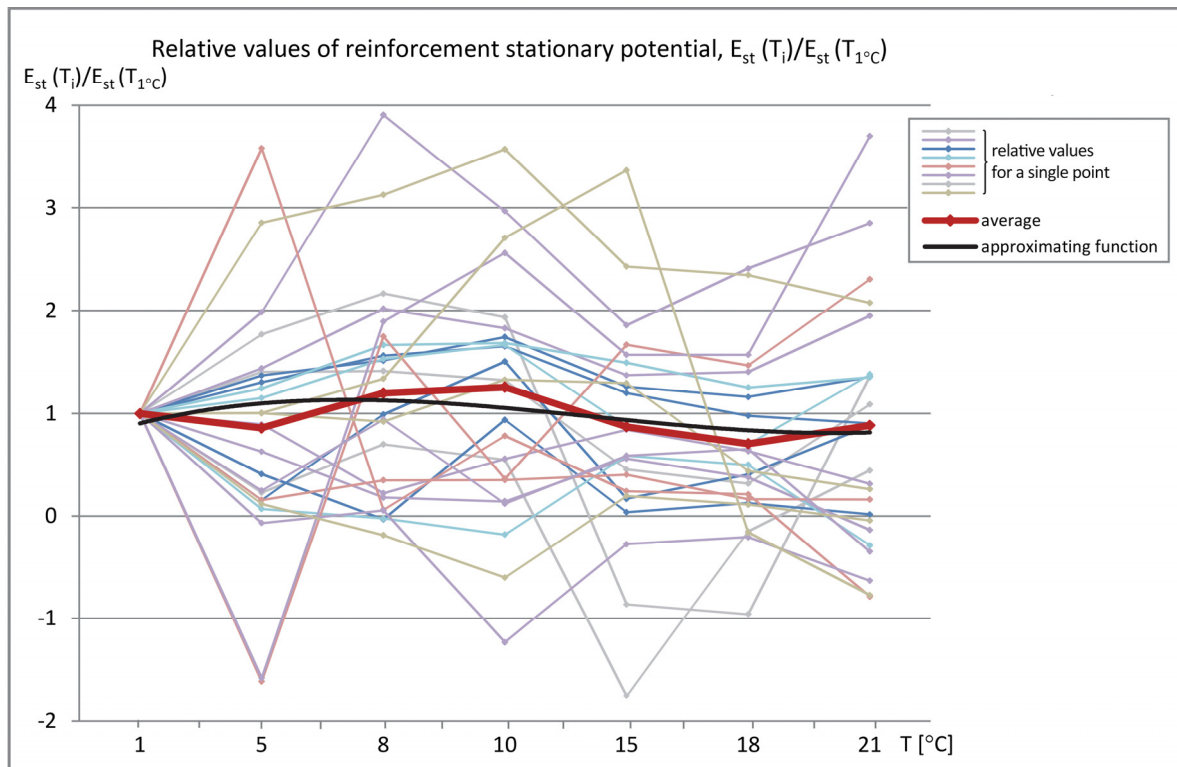
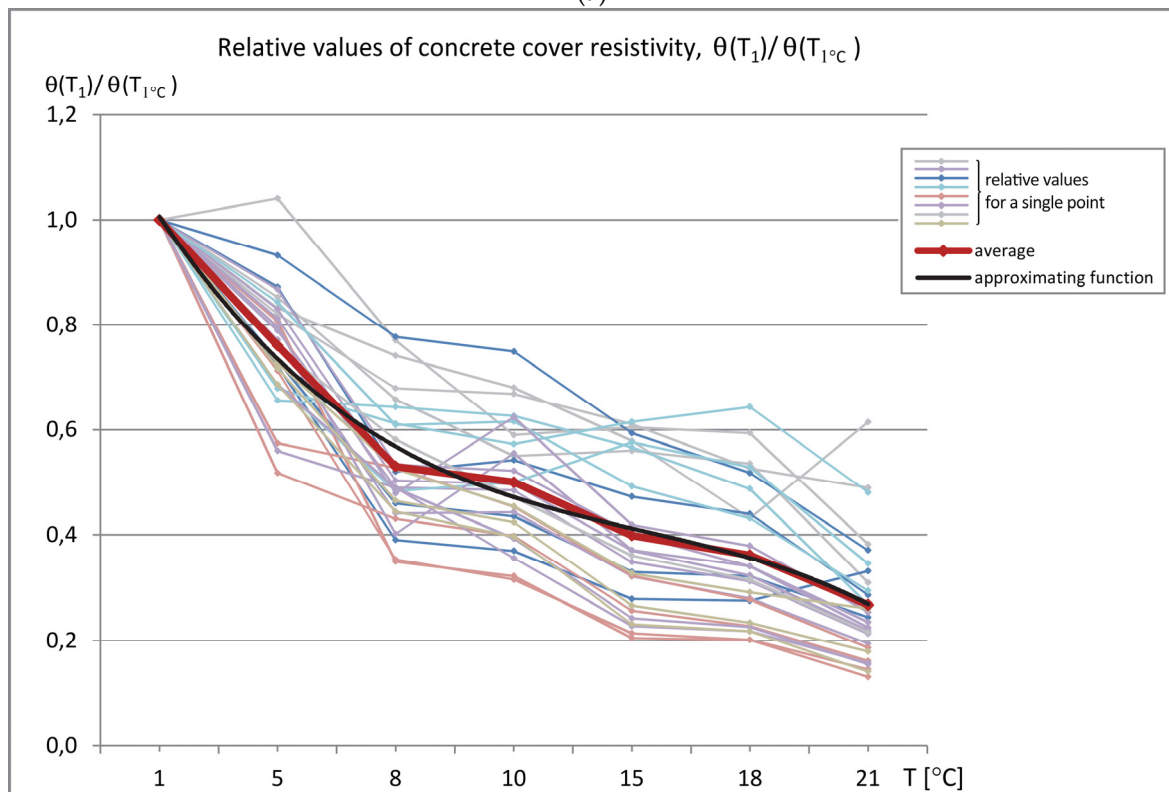


Figure 6. Parameter values measured on specimens at various temperatures; (a) reinforcement stationary potential, (b) concrete cover resistivity, (c) corrosion current density.

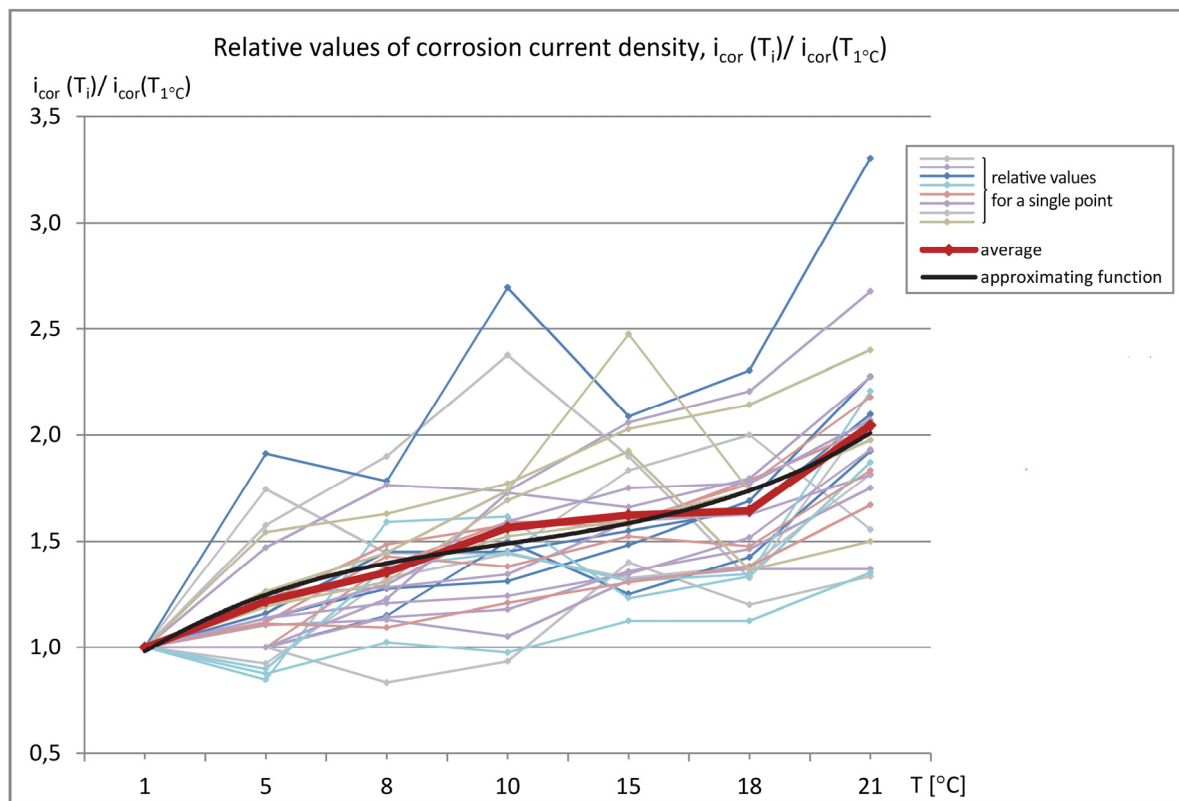


(a)



(b)

Figure 7. Cont.



(c)

Figure 7. Relative values of measured parameters on samples at different temperatures; (a) reinforcement stationary potential, (b) concrete cover resistivity, (c) corrosion current density.

The average value of the reinforcement stationary potential noticeably dropped with the increase in temperature of the tested specimen. The plot of the absolute value changes ranged from $E_{st} \approx 0$ mV at $T = 1$ °C to $E_{st} \approx -77$ mV at $T = 21$ °C. These changes are not strictly monotonic and they are in the range of insignificant values (Figure 6a).

The changes in the concrete cover resistivity values were more explicit and unidirectional. The average value decreased from $\Theta \approx 41$ k Ω ·cm at $T = 1$ °C to $\Theta \approx 10$ k Ω ·cm at $T = 21$ °C. The graph does not differ significantly from the linear one (Figure 6b).

Changes in the average corrosion current density values were also proportional to changes in specimen temperature and ranged from $i_{cor} \approx 0.36$ μ A/cm² at $T = 1$ °C to $i_{cor} \approx 0.72$ μ A/cm² at $T = 21$ °C.

To assess changes in the values of the measured parameters (E_{st} , i_{cor} , Θ) obtained at different temperatures, the plots of relative values were prepared. All of the values were referred to those that were obtained at $T = 1$ °C chosen in this case as the reference temperature. This approach gives the possibility to correct the results in the case of need to compare them with the results that were obtained during measurements performed in different conditions, e.g., in different seasons.

The observed relatively small changes in the average relative values of the reinforcement stationary potential E_{st} are visible in Figure 7a. The positive and negative values of this parameter disturb general analysis of the relative values. It should be remembered that, in in-situ studies, only negative values represent a reliable and significant range of results. Values that are greater than $E_{st} = -200$ mV indicate very low corrosion probability. Therefore, the trend of changes as a function of temperature was verified on specimens with advanced reinforcement corrosion and presented in a separate publication.

The average value of the concrete cover resistivity (Θ) at higher temperatures clearly decreases down to 25% of the value at $T = 1$ °C. As the changes are significant, the inference about the corrosion risk of the tested element will be different.

The most important factor enabling the determination of the reinforcement corrosion activity, i.e., the corrosion current density (i_{cor}) changed by ~100% at the temperature $T = 21\text{ }^{\circ}\text{C}$ in relation to the reference temperature (i.e., $T = 1\text{ }^{\circ}\text{C}$). While the absolute values, regardless of the temperature, were insignificant and indicated low reinforcement corrosion activity, the observed relative changes of the i_{cor} values in relation to those that were measured at the reference temperature are considerable. Therefore, the prediction of the reinforcement corrosion activity requires taking into account the temperature of the element being tested. Otherwise, the measurement will be inaccurate.

There were extreme differences in the relative values of the measured parameters at individual points in relation to the average values at these points: the reinforcement stationary potential - Est $\pm 200 \div 500\%$, the concrete cover resistivity - $\Theta \pm 40 \div 85\%$, and the corrosion current density - $i_{\text{cor}} \pm 25 \div 300\%$.

5. Conclusions

The tests confirmed the effect of temperature on the assessment of reinforcement corrosion risk in concrete by the galvanostatic pulse method. The differences in the values of the reinforcement stationary potential, concrete cover resistivity, and corrosion current density, measured on the same specimens but at different temperatures, in some cases amounted to several dozen percent. This means that measurements of real structural elements made while using the GPM at different temperatures (seasons) can lead to incorrect estimation of the probability of reinforcement corrosion in the examined area and the incorrect assessment of its corrosion activity over time. Therefore, it is advisable to specify the appropriate temperature correction factors for measurements made while using the GPM. The authors' intention is to estimate the value of the necessary correction factors.

Author Contributions: Conceptualization, W.R. and A.W.; methodology and tests, W.R. and A.W.; formal analysis, W.R. and A.W.; data interpretation, W.R. and A.W.; writing—Original draft preparation, W.R. and A.W.; editing, W.R.; funding acquisition, W.R. and A.W. All authors have read and agreed to the published version of the manuscript.

Funding: This research was funded by grant number 02.0.06.00/2.01.01.01. 0007; MNSP. BKWB. 16.001 "Analysis of limit states, durability and diagnostics of structures and methods and tools for quality assurance in construction" [Kielce University of Technology, Kielce, Poland].

Conflicts of Interest: The authors declare no conflict of interest.

References

1. EN 1992-1-1:2008 Eurocode 2. *Design of Concrete Structures. Part 1-1: General Standard and Standards for Buildings*; Polish Committee for Standardization: Warsaw, Poland, 2008.
2. Neville, A.M. *Properties of Concrete*, 5th ed.; Pearson: London, UK, 2011.
3. Tang, S.W.; Yao, Y.; Andrade, C.; Li, Z.J. Recent durability studies on concrete structure. *Cem. Concr. Res.* **2015**, *78 Pt A*, 143–154. [[CrossRef](#)]
4. Baltazar-Zamora, M.A.; Bastidas, D.; Santiago-Hurtado, G.; Mendoza-Rangel, J.M.; Gaona-Tiburcio, C.; Bastidas, J.M.; Almeraya-Calderón, F. Effect of Silica Fume and Fly Ash Admixtures on the Corrosion Behavior of AISI 304 Embedded in Concrete Exposed in 3.5% NaCl Solution. *Materials* **2019**, *12*, 4007. [[CrossRef](#)] [[PubMed](#)]
5. Gjrrv, O.E. Durability of Concrete Structures. *Arab. J. Sci. Eng.* **2011**, *36*, 151–172. [[CrossRef](#)]
6. Drobiec, Ł.; Jasiński, R.; Piekarczyk, A. *Diagnosis of Reinforced Concrete Structures. Methodology, Field and Laboratory Testing of Concrete and Steel*, 1st ed.; PWN: Warsaw, Poland, 2010.
7. Luo, D.; Li, Y.; Li, J.; Lim, K.S.; Nazal, N.A.M.; Ahmad, H. A Recent Progress of Steel Bar Corrosion Diagnostic Techniques in RC Structures. *Sensors* **2018**, *19*, 34. [[CrossRef](#)] [[PubMed](#)]
8. Jaśniok, M.; Jaśniok, T. Measurements on corrosion rate of reinforcing steel under various environmental conditions, using an insulator to delimit the polarized area. *Procedia Eng.* **2017**, *193*, 431–438. [[CrossRef](#)]
9. Verma, S.K.; Bhadauria, S.S.; Akhtar, S. Monitoring Corrosion of Steel Bars in Reinforced Concrete Structures. *Sci. World J.* **2014**, *2014*. [[CrossRef](#)] [[PubMed](#)]

10. Raczkiwicz, W.; Kossakowski, P.G. Electrochemical Diagnostics of Sprayed Fiber-Reinforced Concrete Corrosion. *Appl. Sci.* **2019**, *9*, 3763. [[CrossRef](#)]
11. Schabowicz, K. Non-destructive testing of materials in civil engineering. *Materials* **2019**, *12*, 323. [[CrossRef](#)] [[PubMed](#)]
12. Hoła, J.; Schabowicz, K. State-of-the-art non-destructive methods for diagnostic testing of building structures—anticipated development trends. *Arch. Civ. Mech. Eng.* **2010**, *10*, 5–18. [[CrossRef](#)]
13. Stankiewicz, H. (Ed.) *Corrosion Protection Technique. Sec. XI: Corrosion and Resistance of Mineral Materials*; PWSZ: Warsaw, Poland, 1973.
14. Kurdowski, W. *Cement and Concrete Chemistry. Industrial Chemistry and Chemical Engineering*; Springer: Berlin/Heidelberg, Germany, 2014.
15. Bertolini, L.; Elsener, B.; Pedferri, P.; Polder, R. *Corrosion of Steel in Concrete*, 2nd ed.; Wiley VCH: Weinheim, Germany, 2004.
16. Chess, P.; Green, W. *Durability of Reinforced Concrete Structures*, 1st ed.; CRC Press: Boca Raton, FL, USA, 2019.
17. Brodnan, M.; Kotes, P.; Vanerek, J.; Drochytka, R. Corrosion Determination of Reinforcement Using The Electrical Resistance Method. *Materialiin Tehnologije* **2017**, *51*, 85–93. [[CrossRef](#)]
18. Brodnan, M.; Koteš, P.; Bahleda, F.; Šebök, M.; Kučera, M.; Kubissa, W. Using non-destructive methods for measurement of reinforcement corrosion in practice. *Prot. Against Corros.* **2017**, *21*, 55–58.
19. Morris, W.; Vico, A.; Vazquez, M.; de Sanchez, S.R. Corrosion of reinforcing steel evaluated by means of concrete resistivity measurements. *Corros. Sci.* **2002**, *44*, 81–99. [[CrossRef](#)]
20. Østvik, J.-M. Thermal Aspects of Corrosion of Steel in Concrete: Effect of Low Temperature on the Resistivity and the Cathodic Reaction Rate. Ph.D. Thesis, Norwegian University of Science and Technology, Trondheim, Norway, 2005.
21. Raczkiwicz, W.; Wójcicki, A.; Grzmil, W.; Zapala-Slaweta, J. Impact of Environment Conditions on the Degradation Process of Selected Reinforced Concrete Elements. IOP Conference Serie—Materials Science and Engineering. In Proceedings of the 3rd World Multidisciplinary Civil Engineering, Architecture, Urban Planning Symposium (WMCAUS 2018), Prague, Czech Republic, 18–22 June 2018; IOP: London, UK, 2019; Volume 471. [[CrossRef](#)]
22. Bäßler, R.; Burkert, A.; Frølund, T.; Klinghofer, O. Usage of GPM-Portable equipment for determination of corrosion stage of concrete structures. *Corrosion* **2003**, 03388.
23. Frølund, T.; Jensen, F.M.; Bäßler, R. *Smart Structures: Determination of Reinforcement Corrosion Rate by Means of the GPT*; IABMAS Congress: Barcelona, Spain, 2002.
24. Sørense, H.E.; Frølund, T. Monitoring of reinforcement corrosion in marine concrete structures by the GPM. In Proceedings of the International Conference on Concrete in Marin Environments, Hanoi, Vietnam, October 2012; pp. 213–220. [[CrossRef](#)]
25. Raczkiwicz, W.; Wójcicki, A. Selected aspects of forecasting the level of reinforcing steel corrosion in concrete by electrochemical method. *Weld. Rev.* **2017**, *89*, 28–33.
26. Elsener, B.; Klinghoffer, O.; Frølund, T.; Rislund, E.; Schiegg, Y.; Böhni, H. Assessment of reinforcement corrosion by means of galvanostatic pulse technique. In Proceedings of the International Conference—Repair of Concrete Structures, Svolvaer, Norway, 28–30 May 1997.
27. Frølund, T.; Klinghofer, O.; Poulsen, E. *Rebar Corrosion Rate Measurements for Service Life Estimates*; ACI Fall Convention: Toronto, ON, Canada, 2000.
28. Raczkiwicz, W.; Wójcicki, A. Evaluation of effectiveness of concrete coat as a steel bars protection in the structure—galvanostatic pulse method. In Proceedings of the 26th International Conference On Metallurgy And Materials (METAL), Brno, Czech Republic, 24–26 May 2017.
29. Raczkiwicz, W.; Grzmil, W. Assessment of the impact of cement type on the process of concrete carbonation and reinforcement corrosion in reinforced concrete specimens. *Cem. Lime Concr.* **2017**, *4*, 311–319.
30. Vedalakshmi, R.; Balamurugan, L.; Saraswathy, V.; Kim, S.-H.; Ann, K.Y. Reliability of Galvanostatic Pulse Technique in assessing the corrosion rate of rebar in concrete structures: Laboratory vs field studies. *Ksce J. Civ. Eng.* **2010**, *14*, 867–877. [[CrossRef](#)]

31. Allampallewar, S.B.; Srividya, A. Corrosion performance of reinforced concrete member along Indian coasts: Effect of temperature & relative humidity. *Int. J. Perform.* **2008**, *4*, 285–292.
32. Available online: <http://www.germann.org/TestSystems/GalvaPulse/GalvaPulse.pdf> (accessed on 28 September 2019).



© 2020 by the authors. Licensee MDPI, Basel, Switzerland. This article is an open access article distributed under the terms and conditions of the Creative Commons Attribution (CC BY) license (<http://creativecommons.org/licenses/by/4.0/>).